Quantification of leaf-scale light energy allocation and photoprotection processes in a Mediterranean pine forest under extensive seasonal drought

Running title: Photoprotection and energy allocation under seasonal drought

Kadmiel Maseyk[1,3], Tongbao Lin[1,4], Amnon Cochavi[1], Amnon Schwartz[2] and Dan Yakir[1]

[1] Department of Earth and Planetary Science, Weizmann Institute of Science, Rehovot 76100, Israel

[2] Robert H. Smith Institute of Plant Sciences and Genetics in Agriculture, Faculty of Agricultural, Food and Environmental Quality Sciences, the Hebrew University of Jerusalem, Rehovot, Israel.

[3] Present address: School of Environment, Earth and Ecosystem Sciences, The Open University, Milton Keynes MK7 6AA, United Kingdom.

[4] Present address: College of Agronomy, Henan Agricultural University, Zhengzhou 450002, Henan, P.R. China

*Corresponding author: dan.yakir@weizmann.ac.il

Keywords: Aleppo pine, Mediterranean ecosystem, photoinhibition, carotenoids, drought resilience

Abstract

Photoprotection strategies in a *Pinus halepensis* forest at the dry timberline that shows sustained photosynthetic activity during 6-7 months summer drought were characterized and quantified under field conditions. Measurements of chlorophyll fluorescence, leaf-level gas exchange and pigment concentrations were made in both control and summer-irrigated plots, providing the opportunity to separate the effects of atmospheric from soil water stress on the photoprotection responses. The proportion of light energy incident on the leaf surface ultimately being used for carbon assimilation was 18% under stress-free conditions (irrigated, winter), declining to 4% under maximal stress (control, summer). Allocation of absorbed light energy to photochemistry decreased from 25 to 15% (control) and from 50% to 30% (irrigated) between winter and summer, highlighting the important role of pigment-mediated energy dissipation processes. Photorespiration or other non-assimilatory electron flow accounted for 15-20% and less than 10% of incident light energy during periods of high and low carbon fixation, respectively, representing a proportional increase in photochemical energy going to photorespiration in summer but a decrease in the absolute amount of photorespiratory CO_2 loss. Resilience of the leaf photochemical apparatus was expressed in the complete recovery of photosystem II efficiency (Φ_{PSII}) and relaxation of the xanthophyll de-epoxidation state (DPS) on the diurnal cycle throughout the year, and no seasonal decrease in pre-dawn maximal photosystem II efficiency (F_v/F_m). The response of CO_2 assimilation and photoprotection strategies to stomatal conductance and leaf water potential appeared independent of whether stress was due to atmospheric or soil water deficits across seasons and treatments. The range of protection characteristics identified provide insights into the relatively high carbon economy under these dry conditions, conditions which are predicted for extended areas in the Mediterranean and other regions due to global climate change.

Introduction

Water stress, in terms of both soil water availability and atmospheric vapour pressure deficits (*D*), is a key limitation to plant productivity (Boyer 1982, Novick et al. 2016). Consistent features of climate change predictions are a decrease in summer rainfall and an increase in evaporative demand, increasing the drought risk and drought frequency across many areas globally, including the Mediterranean Basin (Naumann et al. 2018). The response of plants adapted to warm and dry conditions can provide valuable insights into growth under drought conditions (Peñuelas et al. 2001, Flexas and Medrano 2002, Grünzweig et al. 2003, Garcia-Plazaola et al. 2008, Maseyk et al. 2008a, Maseyk et al. 2008b, Raz-Yaseef et al. 2010, Grossiord et al. 2017), and are essential for reliable assessments of vegetation dynamics under future climate scenarios (Breshears et al. 2005, Combourieu-Nebout et al. 2015, Adams et al. 2017).

The combination of high irradiance and stomatal closure during drought brings the risk of damage to the photosynthetic apparatus due to the over-reduction of the photosynthetic apparatus. The excess of electrons forms reactive oxygen species that can cause protein damage and membrane peroxidation (Smirnoff 1993, Long et al. 1994). Protection strategies against oxidative damage include mechanisms that reduce energy transfer to the photosystems, provide alternative sinks for photochemical energy to CO_2 fixation and systems for scavenging active oxygen species. Pigment mediated processes include a reduction in chlorophyll to reduce the initial solar energy absorption (Kyparissis et al. 1995, Elvira et al. 1998) and the synthesis of carotenoid pigments, including carotenes and xanthophylls (Demmig-Adams 1990, Tracewell et al. 2001). An important energy dissipation process involves the de-epoxidation of violaxanthin (V) via antherxanthin (A) to zeaxanthin (Z) in the highly dynamic xanthophyll cycle, and non-radiative (thermal) dissipation of energy (Demmig et al. 1987, Demmig-Adams and Adams 2006). The process of photorespiration, or

other non-assimilatory electron flow such as the Mehler-peroxidase pathway, while typically considered a cost to plant carbon balance, provides an additional sink for photochemical energy, facilitating continual electron flow through the electron transport system and serving to maintain photosystem functionality under drought and other stressful conditions (Kozaki and Takeba 1996, Wingler et al. 2000, Eisenhut et al. 2017).

While these various photoprotection responses during drought have been well documented in controlled and, to a lesser extent, field studies, systematic analysis and quantification of the relative contribution of the various pathways under natural conditions remain rare (Valentini et al. 1995, Flexas and Medrano 2002, Beis and Patakas 2012). Furthermore, the relative importance of the different processes may depend on the functional plant type and the nature of the stress (Demmig-Adams and Adams 2006), with a shift from more flexible and reversible xanthophyll cycle processes to more sustained dissipation under prolonged stress. In this context, the effects of high vapour pressure deficits and low soil water contents may induce different responses, and recent studies have demonstrated the importance of high atmospheric VPD even without low soil moisture content on tree physiology (Novick et al. 2016, Grossiord et al. 2017). Atmospheric vapour pressure deficits, while showing an average increase through summer, can have high daily and synoptic scale variations that result in more transient and short-term effects on photosynthetic capacity. Increasing soil water deficits, on the other hand, reduce g_s and A in a progressive manner resulting in lowered photosynthetic capacity over a prolonged period of time.

In this study, we present results of a field study that quantified the role of primary photochemical protection strategies in mature *Pinus halepensis* Mill. (Allepo pine) at the arid limit of the Mediterranean climate region (Grünzweig et al. 2003). *P. halepensis* is a highly drought tolerant species (Schiller 2000) that is a key species of the Mediterranean region, with an extensive natural distribution (Quézel 2000) and widespread use in reforestation and land

reclamation efforts (Pausas et al. 2004). Even at the arid limit of distribution, it has been shown that ongoing photosynthetic activity during extensive summer drought contributes to both new needle growth (Klein et al. 2005, Maseyk et al. 2008b) and the relatively high productivity observed in this forest (Grünzweig et al. 2003, Maseyk et al. 2008a, Rotenberg and Yakir 2010). Therefore, understanding the role of the various photoprotection mechanisms in this system can provide valuable insight into the successful adaptation of evergreen species to warm and dry conditions. Measurements were made on both summer-irrigated (alleviating dry-season soil moisture deficit but maintaining high atmospheric VPD) and non-irrigated trees (high soil moisture deficit combined with high atmospheric VPD during the dry season) through wet and dry seasons, providing an opportunity to better identify the interactions of high irradiance and temperature with moisture stress in the soil or in the atmosphere.

Materials and Methods

Site description and meteorological measurements

The study was conducted in a 2800 ha mature (35-40 yr old) *P. halepensis* forest in southern Israel (31˚21' N, 35˚ 03' E, 650 m a.s.l.) and spanned two dry and one wet season (from June 2001 to October 2002). The forest is located in a transitional climate zone between the Mediterranean and semi-arid climates and experiences long hot rain free periods of up to ~ 8 months over summer and an average annual rainfall of ~280 mm in a wet season generally between November and March. Tree density was 300 - 350 trees ha^{-1}, mean tree height 10 m and leaf area index 1.5, on a shallow soil (0.2-1 m deep Rendzina above chalk and limestone) with a deep (~300 m) ground water table (Grünzweig et al. 2007). Measurements of meteorological parameters and carbon and water fluxes have been made at the forest since 2001 (Grünzweig et al. 2003), and show that annual evapotranspiration closely balances

precipitation and the aridity index (ratio of precipitation to potential evapotranspiration) is ~0.18, typical of arid regions (Raz-Yaseef et al. 2010). Monthly mean daytime air temperatures range between 11.2 ± 2.0˚C (Jan) and 28.3 ± 0.9 ˚C (Aug). Soil water content reaches field capacity during the wet season and declines to below 10% (volumetric) during the rain free period. Measurements of photosynthetically active radiation (PAR), air temperature, vapour pressure deficit (*D*) and precipitation monitored continuously 5 m above the canopy at the flux site (within 1 km from the study site) for the study period are shown in Fig. 1.

Irrigation treatment

Starting in May 2001, supplementary summer-time irrigation was provided to a plot of 15 trees in order to maintain soil water at close to field capacity throughout the year (Klein et al. 2005). Drip irrigation was provided around the base of the trees at a rate of 3.4-4.0 mm day^{-1} for the two dry seasons, but was reduced once natural precipitation resumed in the intervening autumn, was suspended over winter once the non-irrigated soil had reached field capacity, and resumed according to rainfall intensity in spring. Trees adjacent to the irrigated plot, but receiving no influence of the irrigation, were used as control non-irrigated trees.

Needle gas exchange

Measurements of projected area based (from measured needle widths) needle net photosynthetic rates (*A*), leaf transpiration (*E*) and stomatal conductance to water vapour (g_s) were measured *in-situ* with an LI-6400 photosynthesis system as described in Maseyk et al. (2008b). Diurnal patterns of needle gas exchange were made on relatively cloud-free days on ten occasions over the course of the study period. Needle growth occurs during April – October, and the first measurements on the current year needles were made in late May or

June, when needles were about 50% of their final length. Needles of this age class were designated *y*0 needles, and the older age class (previous year needles) were designated *y*1 needles (*P. halepensis* generally retains 2 - 4 age cohorts of needles on the tree). Needles remained in their age class until the first measurements on the new needles the following year. Measurements were made on the two youngest (*y*0 and *y*1) age classes of needles on 4-6 trees from both the irrigated and control group 5-6 times over the course of the photoperiod, maintaining ambient conditions of temperature, relative humidity, PAR and CO_2 concentration in the leaf cuvette.

Chlorophyll fluorescence and energy partitioning

Chlorophyll *a* fluorescence measurements were made in parallel to the gas exchange measurements on the same needle cohort, using a pulse modulated excitation and detection fluorometer (PAM-2000 Portable Fluorometer, Heinz Walz GmbH, Germany). Measurements were made on a group of attached needles, aligned parallel to each other in the probe clip, using the saturation pulse technique. Needles were maintained in their aligned arrangement during the day by lightly clamping them with toothpicks, and the fluorescence probe clip was centred on the aligned needles to ensure that repeat measurements were made on the same needle area and at the same distance from the needles. Fluorescence yields that were monitored included the minimum and maximum yield with full closure of photosystem II (PSII) reaction centres (following application of the saturation pulse) in the dark-adapted state (F_o and F_m, respectively, measured predawn) and steady-state, minimum and maximum yields the light adapted state (F', F_o' and F_m', respectively). To determine the minimal fluorescence yield of a pre-illuminated sample (F_o'), the sample was briefly shaded with a black cloth following the saturation pulse and F_m' determination to exclude ambient light, followed by a brief application of far-red light (peak of about 735 nm) to excite photosystem I only and re-

oxidise photosystem II quinine acceptors (Q_A). The steady state F_o' was then recorded while the far-red light was on. The fluorescence signals were monitored graphically in real-time to ensure steady-state levels of F_o, F and F_o'. When F_m' was reduced to low levels that made it difficult to separate from the signal noise of F (e.g. at midday under high light), the measuring beam frequency was increased from the standard setting of 600 Hz to 20 kHz just prior to applying the saturation pulse.

The maximum quantum efficiency of electron transport through PSII to Q_A was determined from the predawn measurements as F_v/F_m, where $F_v = F_m - F_o$. In the light acclimated state, light energy absorbed by the photosystem antenna was partitioned between photochemistry and non-photochemical quenching processes. The effective quantum efficiency of PSII in the light acclimated state (Φ_{PSII}) was determined as (Genty et al. 1989):

$$\phi_{PSII} = \frac{F_m' - F'}{F_m'}. \qquad \text{Eq. 1}$$

Based on a 'lake model' of interconnected reaction centres and antenna matrix, the quantum efficiencies of non-photochemical processes can be partitioned into those associated with constitutive non-light induced thermal dissipation (Φ_{NO}) and the regulated thermal non-photochemical dissipation (Φ_{NPQ}) as (Kramer et al. 2004):

$$\phi_{NO} = \frac{1}{NPQ + 1 + q_L (F_m / F_o - 1)}, \qquad \text{Eq. 2}$$

and, because the sum of Φ_{PSII}, Φ_{NO} and Φ_{NPQ} is unity:

$$\phi_{NPQ} = 1 - \phi_{PSII} - \phi_{NO}, \qquad \text{Eq. 3}$$

where NPQ = $(F_m - F_m')/F_m'$ describes the reduction, or quenching, of maximal fluorescence between the dark and light states due to non-photochemical processes, and $q_L = (F_m' - F')/(F_m' - F_o')\cdot(F_o'/F')$ is the fraction of Q_A in the oxidised state (open reaction centres). The fractional allocation of absorbed light energy between Φ_{PSII}, Φ_{NPQ} and Φ_{NO} was estimated at midday on

198 a number of days through the study period, and for the entire diurnal cycle on days with
199 sufficient data.

200 From the values of Φ_{PSII}, estimates of the non-cyclic electron transport rate (in μmol e^-
201 m^{-2} s^{-1}) through PSII can be made according to:

202 $$ETR = \phi_{PSII} \times I \times 0.5 \times \alpha \qquad \text{Eq. 4}$$

203 where I is the level of PAR incident on the leaf, α is leaf absorbance and 0.5 is the estimate of
204 the fraction of absorbed light received by PSII (i.e. assuming an equal distribution between
205 PSI and PSII). Estimates of leaf absorbance were made from measurements of chlorophyll
206 content (see below), following Evans and Poorter (2001):

207 $$\alpha = \chi/(\chi + 76) \qquad \text{Eq. 5}$$

208 where χ is chlorophyll content per unit leaf area (μmol m^{-2}).

209 Similarly, the rate of energy dissipation via regulatory thermal processes (TDR) is:

210 $$TDR = \phi_{NPQ} \times I \times \alpha \qquad \text{Eq. 6}$$

211

212 *Photorespiration rates*

213 From the relationship between PSII electron transport rates (ETR) and CO_2 assimilation (A),
214 rates of photorespiratory CO_2 release (R_l) can be calculated according to Valentini et al.
215 (1995):

216 $$R_l = J_o/8 \qquad \text{Eq. 7}$$

217 where J_o is the rate of electron flow to photorespiration, and is calculated as:

218 $$J_o = 2/3(ETR - 4(A + R_d)) \qquad \text{Eq. 8}$$

219 where R_d is the rate of needle dark respiration, measured at the end of the day after sunset.
220 Estimates of the allocation of photochemical energy to photorespiration were made from

measurements of gas exchange and chlorophyll fluorescence around midday when PAR > 1000 μmol m^{-2} s^{-1}.

Chlorophyll and carotenoid content

On select days in 2002, mature needle samples were collected for chlorophyll and carotenoid content determination from 3 trees of each treatment at 6 points in the photoperiod. The samples were immediately frozen in liquid nitrogen and kept at -70°C until the analysis. The samples were homogenized with a pestle and mortar and the pigments were extracted from the homogenate in a cold room and under dim light. The extracts were centrifuged at 4000*g* to remove cell debris and the supernatant was filtered through a 0.45μm mesh filter. Chlorophyll was extracted in 80% acetone (v/v) and chlorophyll concentration was determined spectrophotometrically. The carotenoid pigments (xanthophylls V, A, Z, lutein (L) and neoxanthin (N) and α- and β-carotene) were extracted twice with 90% acetone and analyzed by HPLC (Merck Hitachi 6200) equipped with a diode array detector. The compounds were separated on a LiChrospher 100 RP-18 (4×250 mm, 5μm) HPLC column using the following acetone/water (a/w) gradient: from 0 to 3 min a/w was isocratically maintained at 40/60, then the percent of acetone was linearly increased in from 40% to 95% over 20 min, and finally the column was washed with a/w 95/5 for 10 min. The flow rate was 1 ml/min and the volume of injection was 20 μl. The pigments were identified by co-chromatography with standards obtained from DHI Water and Environment (Horsholm Denmark).

Branch water potential

Plant water status was monitored by measuring the predawn (Ψ_{PD}) and midday (Ψ_{MD}) water potential on apical twigs containing the *y*0 and *y*1 needle cohorts from the same trees as the gas exchange and florescence measurements. The measurements were made using a

246 Scholander-type pressure chamber (Arimad 2, A.I.R., Kfar-Charuv, Israel) with moist paper
247 inside to avoid humidity changes during measurement.
248
249 *System-level incident PAR energy allocation*
250 To provide an integrated leaf-level view of the PAR energy allocation strategies across the
251 various pathways and sinks detailed above, we provide a system summary that compares
252 allocation under low stress and maximal CO_2 assimilation rates (irrigated trees in spring and
253 winter) with allocation under maximal stress and minimal CO_2 assimilation rates (summer in
254 the control trees). The proportion of incident PAR absorbed by the leaf was calculated from
255 chlorophyll content (Eq. 5), with the balance being either transmitted or reflected. The
256 distribution of this absorbed PAR between photochemistry, constitutive and regulated thermal
257 dissipation was calculated from Equations 1 – 3, and the distribution of photochemical energy
258 between CO_2 assimilation and photorespiration was determined from the measurements of A
259 and calculations of R_l (Eq. 7 and 8).
260
261 *Statistical analyses*
262 Statistical differences in pre-dawn F_v/F_m values and the daily energy allocation between
263 control and irrigated trees was tested for using unpaired non-directional t-tests of the daily
264 mean values on the day of measurement. The tests were only conducted between control and
265 irrigated trees for the measurement day, under the null hypothesis assumption of a difference
266 in means of 0, and not between different days within the season (either within or between
267 treatments). Statistical analyses were performed using R version 3.5.3 "Great Truth" (The R
268 Foundation for Statistical Computing, 2016). Linear regression and curve fitting analysis was
269 performed using Origin data analysis and graphing software (OriginLab Corporation,
270 Northampton, Massachusetts, USA).

Results

Meteorological conditions and plant water status

The environmental conditions over the study period were typical for this site (Fig. 1). Mean daytime air temperature was about 28°C in July and August and dropped to 5-10°C in January, with maximum daytime temperatures reaching 35-40°C in summer. Mean daytime *D* often reached values of 4000 Pa or more over summer. Rainfall for the 2001-02 wet season was ~10% above average at 313 mm but was within one standard deviation (88 mm) of the long-term mean.

The irrigation treatment was effective at relieving soil water stress, as Ψ_{PD} values in the irrigated trees were stable over the study period and similar to those in the control trees in the wet months (-0.8 to -1.2 MPa in December – March, Fig. 1e). During the summer drought period Ψ_{PD} values in the non-irrigated trees declined to values of -2.3 MPa, when summer time volumetric soil water contents in the forest reach ~8%. The lowest (summer time) Ψ_{MD} values were -2.7 MPa and -2.4 MPa in the control and irrigated trees, respectively, while Ψ_{MD} was highest and similar between treatments at about -2.3 MPa in March.

Net CO_2 assimilation patterns

Diurnal and seasonal patterns of net CO_2 assimilation (*A*) in the control trees (Fig. 2a,b) were consistent with those described for this forest site (Maseyk et al. 2008b). There was persistence of photosynthetic activity throughout the year, but rates were greatly reduced in the non-irrigated trees in summer and autumn, with midday depressions confining net leaf-level carbon gain to the early morning and late afternoon (e.g. Aug'02 in Fig. 2a). Assimilation rates in the irrigated trees exceeded those in the control trees for much of the year but rates were still lower in summer relative to winter despite the high soil water

availability. Results from biweekly measurements of gas exchange throughout the season made during the hours of peak activity showed that the control and irrigated trees had similar photosynthetic rates for the period between January to April, when annual photosynthesis was maximal (rates of ~18 μmol m^{-2} s^{-1}, results not shown, but see March 2002 in Table 1). Daily maximal photosynthetic rates and total leaf-level CO_2 assimilation during the photoperiod (from integration of the diurnal assimilation data) were reduced by up to 95% in summer in the control trees relative to the winter-spring maximum, while in the irrigated trees the summer rates were reduced by up to 50% (Table 1). Assimilation rates in both control and irrigated trees were closely coupled with stomatal conductance (Fig. 3) and a robust relationship between A and g_s ($A = -0.634 + 18.14(1 - e^{-8.0*gs})$, $r^2 = 0.94$) was evident across the data of both treatments over the range of temporal scales (diurnal and seasonal), climatic parameters (e.g. D, temperature and irradiance; Fig. 1) and needle age classes.

Photosystem efficiencies and pigment content

Photosystem II efficiency (Φ_{PSII}) showed characteristic diurnal patterns in both treatments, with a decrease during the morning to a midday minimum as radiation increased, followed by recovery in the afternoon (Fig. 2c,d). The initial points of each Φ_{PSII} curve in Fig. 2 are the pre-dawn, dark-adapted F_v/F_m values, or maximal efficiencies. In all cases the PSII efficiencies had returned to near their pre-dawn values by the end of the photoperiod, and the F_v/F_m values remained high through the seasons in all samples (Table 1). There was no difference in mean F_v/F_m values across the study period between age classes within a treatment (paired sample t-test between age classes on the same individual), but the mean F_v/F_m value was slightly higher in the irrigated trees (0.815 ± 0.012 and 0.827 ± 0.014 in the control and irrigated samples, respectively, for mean ± SD, n=10, significantly different at the 0.05 level, unpaired t-test of treatment means).

Concurrent with the diurnal changes in Φ_{PSII} were changes in the efficiency of regulated thermal dissipation (Φ_{NPQ}) that balanced the changes in Φ_{PSII}, with constitutive dissipation (Φ_{NO}) remaining stable during the day (Fig. 4). Non-photochemical quenching as parameterised by both Φ_{NPQ} and NPQ were similarly correlated with diurnal changes in the de-epoxidation state of the xanthophyll-cycle pigments (DPS = (A+Z)/(V+A+Z), Fig. 4). The coefficients of determination (r^2) values ranged between 0.46 and 0.94 for the relationship between NPQ and DPS (data not shown) and were significant in both treatments for August and October. For all data (treatments and dates combined) the relationships were Φ_{NPQ} = 0.817·DPS + 0.17 (r^2 = 0.63, p<0.0001) and NPQ = 8.86·DPS – 0.15 (r^2 = 0.69, p<0.0001).

Seasonal changes in pigment contents were correlated between the two treatments (Table 2). No clear diurnal patterns were observed in the pigments other than those of the xanthophyll cycle. Both chlorophyll and total carotenoid content was higher in the irrigated trees, but chlorophyll content decreased seasonally in both the irrigated and non-irrigated trees (Table 2). Total chlorophyll content decreased by 53% in the control and by 46% in the irrigated samples between March and August, resulting in reductions in leaf absorbance (α) from 0.87 to 0.76 (control) and from 0.89 to 0.81 (irrigated) between March and October. The total carotenoid content was variable, but also at a minimum in August in both treatments. The carotenoid pigments were evenly divided between the xanthophylls and carotenes in March and May, but the xanthophyll component increased to 86% (control) and 72% (irrigated) in August. Although lutein typically comprised the largest part of the xanthophyll pool (between 40 – 60%), the seasonal xanthophyll increase was driven by a 4 to 5-fold increase in the xanthophyll-cycle pigments (V, A, Z), with similar decreases in the precursor β-carotene. A common relationship between the carotene and xanthophyll components of the carotenoids was present across both treatments, with Xan = 0.67·Car + 0.17 (r^2= 0.82, p = 0.002), where Xan and Car are the total xanthophyll and carotene contents, respectively.

346

347 *Seasonal energy dissipation patterns*

348 Seasonally, the midday (MD) minimum Φ_{PSII} values were lower in the summer than in
349 winter in both treatments and were always lower in the control samples compared to the
350 irrigated plants (Fig. 5), while constitutive dissipation (Φ_{NO}) remained at between 15% - 20%
351 of absorbed irradiance in both treatments through the seasons. The proportion of light
352 absorbed at midday and used in photochemical electron transport declined from 30% in
353 winter to 6% in summer in the control trees, while in the irrigated trees, midday Φ_{PSII}
354 remained at 25 – 30% for much of the year and reached up to 50% in the cooler wet season
355 (Fig. 5). From the days where measurements covered the full diurnal cycle, estimates of the
356 total daily allocation of absorbed energy to the various dissipation pathways were made by
357 weighting the efficiencies at each time step by the incident PAR (Table 1). This weighting
358 provided the actual energy allocation to the various sinks at the integrated daily scale. The
359 whole day allocation to photochemistry in summer was about half of that in winter in the
360 control trees and 60% - 70% of winter values in the irrigated trees, showing less reduction
361 over the diurnal cycle than from the midday measurements. The inversely proportional
362 increases in Φ_{NPQ} relative to the decreases in Φ_{PSII} resulted in ~50% and up to nearly 80% of
363 the daily absorbed energy being dissipated through regulated thermal mechanisms in summer
364 in the irrigated and control trees, respectively. The daily mean values of Φ_{PSII} and Φ_{NPQ} were
365 statistically different between the control and irrigated trees on each day of measurement in
366 the season (Table 1, unpaired t-test between treatment means).

367 The response to incident PAR of electron transport (ETR) and thermal dissipation
368 (TDR) rates derived from the Φ_{PSII} and Φ_{NPQ} data show a separation of the control data into
369 two groups (Fig. 6), one associated with the wet season (Dec – May) and the other the dry
370 season (including early autumn, i.e. June – Nov). ETR were similar between treatments at low

PAR (up to ~300 μmol m^{-2} s^{-1}), above which the rates in the dry period were lower than the wet period and irrigated data (Fig. 6a). The initial slopes of the curves (where response was linear, at PAR less than 100 μmol m^{-2} s^{-1}) were 0.25 ± 0.01, 0.29 ± 0.004 and 0.30 ± 0.006 for the dry season, wet season and irrigated data, respectively. At high PAR (above ~1200 μmol m^{-2} s^{-1}), ETR started to decrease in the dry season. Maximal (light saturated) ETR was about 150 μmol m^{-2} s^{-1} in the wet period and 50-75 μmol m^{-2} s^{-1} in the dry period in the control trees. Maximal ETR in the irrigated trees was quite variable, between about 150 - 250 μmol m^{-2} s^{-1}. TDR rates were about 70% of the incident photon flux at the high light levels in the dry season control trees, compared to about 40-50% in the irrigated trees (Fig. 6b).

Estimates of the rate of photorespiratory CO_2 release (R_l) were calculated from the estimates of non-assimilatory electron flow derived from the values of ETR and gas exchange measurements (Fig. 6c). Overall, photorespiratory CO_2 release was greater in the irrigated trees as a result of the overall higher electron transport rates in the irrigated samples, and again there was similarity between wet season control trees and the irrigated trees. However, photorespiration rates in summer were about half those observed in the wet period in the control trees.

Energy allocation in response to leaf water stress

The proportional allocation of absorbed light energy to photosynthesis, non-assimilatory electron flow or pigment mediated thermal dissipation mechanisms under saturating light have non-linear responses to stomatal conductance (Fig 7). At a stomatal conductance above ~0.1 mol m^{-2} s^{-1} there was little variation in the energy allocation between the pathways, (Fig. 7a-c) and the allocation of total electron transport to non-assimilatory electron flow (J_o/ETR, Fig. 7d). However, at g_s below this apparent critical level there was an increase in thermal dissipation (from ~50 to 70%) resulting in a steep decrease in allocation to CO_2 fixation and a

lesser decrease in the allocation to non-assimilatory electron sinks, such that there was an increase in J_o/ETR. The nature of the response to water potential differs in that the allocation to Rubisco activity was sigmoidal in nature, with a rapid transition between a water potential of -2.3 to -2.5 MPa, while the allocation to thermal dissipation and the J_o/ETR ratio increased more linearly as stress increased.

Combined effects of the various pathways

Combining the effects of the changes in absorption, energy dissipation and allocation of electron transport to carbon or non-assimilatory sinks, estimates were made of the proportion of light incident on the leaf surface that had its fate in the various pathways or sinks. Seasonal values for the allocation to the main sinks of thermal dissipation, CO_2 fixation and photorespiration are shown in Table 1, and a general summary of the stress-dependant seasonal changes between the periods of maximum and minimum CO_2 assimilation is shown in Fig. 8. Around 20% of incident light is reflected or transmitted, following which about 30% is dissipated in the pigment bed under low stress conditions, and up to 50-60% is dissipated thermally under high stress. When conditions for CO_2 fixation are most favourable, 20-30% of incident light is used in photosynthesis, and about half this value is used for photorespiration or other non-assimilatory electron sinks. When water limitation is most severe, only about 5% of incident light energy goes towards carbon assimilation and similar amounts are used in photorespiration.

Discussion

Dynamic energy dissipation maintains stability of the photosynthetic apparatus

Despite the long period of soil water deficit, high vapour pressure deficit and high radiation loads, there were no indications of significant photoinhibitory damage observed in

P. halepensis under either irrigated or non-irrigated conditions. The near complete recovery of Φ_{PSII} by the end of the day (Fig. 2), and long-term stability in F_v/F_m in both control and irrigated trees (Table 1) at values typical of non-stressed plants (*ca*. 0.83; (Björkman and Demmig 1987)), shows there was little cumulative effect of the high light exposure through the long drought period (Baquedano and Castillo 2007). The similarity in the A-g_s response between the treatments (Fig. 3) indicates that the low assimilation rates under the water and atmospheric stress are due primarily to diffusive limitation to gas exchange, rather than metabolic impairment (Flexas et al. 2004, Klein et al. 2011), supporting the view that PSII is relatively stable under drought (Havaux 1992, Cornic 2000).

Overall, the majority of light energy incident on the leaves was excessive to photosynthetic requirements but photosystem integrity was maintained through non-photosynthetic dissipation mechanisms. The main component of the non-photochemical energy dissipation was the light regulated thermal dissipation involving pH mediated xanthophyll-cycle pigments (Figs. 4,5). Constitutive or basal dissipation remained constant (at about 15% of absorbed light), while the regulated thermal dissipation accounted for at least 50% of absorbed light energy during midday in winter, and reached up to ~80% in summer in the control trees. Non-photochemical quenching parameters are known to be correlated with changes in the xanthophyll cycle pigments (Adams III and Demmig-Adams 1994), and we found that both diurnal and seasonal changes in Φ_{NPQ} were highly correlated with xanthophyll-cycle pigment state, and higher levels of xanthophyll cycle pigments were produced in the non-irrigated trees. The low correlation between Φ_{NPQ} and DPS in the irrigated plot during May and October may be attributed to the contribution of different mechanisms of heat dissipation, including proton pumping to decrease the pH gradient from excess light energy (Ruban 2016), thylakoid protein composition, and phosphorylation

(Demmig-Adams et al. 2012), or reuse of excess energy through cyclic electron transport (Kramer and Evans 2011).

Sustained photoinhibition effects can decrease plant productivity and distribution under semi-arid conditions (Werner et al. 2001, Valladares et al. 2005). Investing in a reliance on regulated thermal dissipation over the extensive drought period, rather than increasing basal dissipation, can be advantageous in terms of productivity (Kornyeyev et al. 2004, Murchie and Niyogi 2011, Kromdijk et al. 2016). The stable level of basal dissipation maintains a high potential to utilize energy in photochemistry, and diurnal-scale regulation of pre-PSII energy dissipation enables photochemistry and CO_2 fixation to respond to changes in environmental conditions, including less stressful hours of the day (Fig 2), early or late seasonal rainfall, or milder periods. As an example, average *D* during the August 2001 campaign was 2.9 kPa, compared with 4.1 kPa in 2002 (Fig. 1). Net carbon uptake was maintained throughout the photoperiod in August 2001, but not in 2002 (not shown), resulting in leaf-level carbon gain an order of magnitude higher in 2001 than 2002 (Table 1). The milder conditions could be utilized through maintaining a high potential capacity of the photosystems. The dynamic response of the system can also be seen in the resilience to intense short-term heatwave events (Tatarinov et al. 2016). In this regard, it is interesting to note that the sustained high F_v/F_m and continued reliance on regulated dissipation under these extreme drought conditions contrasts with responses seen to cold winters. Across a range of species and environments, a substantial reduction in F_v/F_m is seen at growth temperatures below 0 ˚C, and this winter photoinhibition is associated with an increase in de-epoxidated state xanthophyll pigments (Míguez et al. 2015). Similarly, during an exceptionally cold winter, a number of Mediterranean evergreen species retained de-epoxidised xanthophylls during the night and showed a sustained decrease in F_v/F_m to values < 0.6 (García-Plazaola et al. 2003).

Both photosystem stability (Damesin and Rambal 1995, Valentini et al. 1995, Faria et al. 1998, Martínez-Ferri et al. 2000, Eppel et al. 2014) and seasonal reductions in photosystem II performance during drought (Faria et al. 1998, Castillo et al. 2002, Llorens et al. 2003, Baquedano and Castillo 2006, Peguero-Pina et al. 2009) have been observed in Mediterranean tree and shrub species. Differences in drought duration and extent of rooting depth (and therefore access to water) may underlie much of the observed differences between species (Faria et al. 1998, Baquedano and Castillo 2007), as can be seen clearly in the difference between the irrigated and control trees in our study. Nevertheless, the non-irrigated trees, growing on shallow soil and experiencing a long period without rain, were able to maintain PSII functionality over the entire summer season, showing a high resistance to long term drought conditions in *P. halepensis*. This low, but continuous, carbon gain sustains leaf development during the long dry summer (Maseyk et al. 2008b) and minimizes plant carbon losses in the photosynthetic 'off-season', contributing to the relatively high annual productivity seen in this system (Grünzweig et al. 2003, Maseyk et al. 2008a).

Reduced role but increased efficiency of photorespiration under high stress

Despite the significant reductions in photochemistry in summer, low stomatal conductance resulted in proportionally greater reductions in net CO_2 assimilation rates and an increase in the proportion of photochemical energy going towards non-assimilatory electron sinks (Fig. 7d). The estimated proportion of non-assimilatory electron flow increased from a minimum of 45% (winter, irrigated) to a maximum of 0.64% (non-irrigated summer) of total electron transport. These values compare to values of 40 – 50% seen in *Quercus cerris* during the Mediterranean summer (Valentini et al. 1995), and are similar to those seen in the desert shrub *Reaumuria soongorica* under severe drought (Bai et al. 2008). These results support an important photoprotection role of non-assimilatory electron flow under drought stress,

495 providing a sink for excess radiation energy and metabolites (glycine, serine) for antioxidant
496 systems (Cornic and Briantais 1991, Wingler et al. 2000, Bai et al. 2008, Beis and Patakas
497 2012).

498 However, the large increase in non-photochemical energy dissipation decreased total
499 electron transport rates between winter and summer (Fig. 6). Consequently, although the
500 relative flux of PSII electron transport to non-assimilatory electron flow increased, the
501 absolute CO_2 loss through photorespiration (R_l) decreased. These results show that as the level
502 of stress increases, greater emphasis on thermal dissipation mechanisms than alternative
503 electron sinks, and the costs involved with increasing thermal dissipation capacity are less
504 than those associated with photorespiration and other non-assimilatory electron sinks. The
505 lower cost in terms of CO_2 but increase in proportional flux through photorespiration shows
506 an increased efficiency in the utilisation of photorespiration for energy dissipation as
507 conductance decreases and temperature increases.

508 Despite the proportionally lower rates of non-assimilatory electron flow,
509 photorespiratory CO_2 loss in summer in the control trees was equivalent to net CO_2 uptake in
510 the less stressful periods, and up to an order of magnitude greater than the concurrent net CO_2
511 uptake. Rates of photorespiratory CO_2 loss have been found to be similar to or exceed net
512 CO_2 uptake in other Mediterranean and savannah species, and may serve to limit leaf carbon
513 balance under high summer irradiances (Valentini et al. 1995, Franco and Lüttge 2002). The
514 rates of photorespiratory CO_2 release were also high in the irrigated trees. In absolute terms,
515 they exceeded the rates from the control trees, and were up to 1.5 – 2 times the rates of
516 irrigated net CO_2 assimilation in summer. We cannot exclude the possibility that
517 photorespiratory CO_2 release was over estimated, and that other non-assimilatory reduction
518 processes, such as the Mehler reaction, serve as important alternative electron sinks (Badger
519 et al. 2000, Flexas and Medrano 2002, Ort and Baker 2002). However, the photorespiration

520 rates are estimated from the residual of net gas exchange and chlorophyll fluorescence
521 measurements and show that, overall, a high proportion of photosystem II electron transport
522 must be accounted for by non-assimilatory electron sinks. The ETR values estimated from the
523 fluorescence data in this study were also consistent with those estimated in this forest from
524 gas exchange CO_2 response curves in a previous study (Maseyk et al. 2008b).
525
526 *Soil-plant-atmosphere hydrological drivers of photoprotection responses*
527 There appears an important stomatal conductance threshold, at around 0.1 mol m^{-2} s^{-1},
528 where the shift in energy allocation patterns occurs. Once stomatal conductance dropped
529 below this threshold was there a marked increase in thermal dissipation and reduction in
530 energy allocation towards Rubisco activity (Fig. 7a-c), and a decrease in electron transport
531 rates and photorespiratory CO_2 release under saturating light (Fig. 6a,c). This observation
532 may support the view that chloroplast CO_2 concentration has an important role in controlling
533 dissipation activity (Flexas and Medrano 2002), and may serve as a basis for mechanistic
534 predications of vegetation responses under drought conditions. However, these changes also
535 occurred when leaf water potential declined below ~-2.3 MPa (fig. 7e-h), in a manner similar
536 to that seen in oaks (Peguero-Pina et al. 2009), and it is difficult to separate the role of these
537 two factors on the observed responses, especially considering their mutual interactions (Klein
538 et al. 2011).
539 The current study also provided a unique opportunity to separate possible effects of
540 the more gradual changes of combined soil and atmospheric water stress (control trees) from
541 the more dynamic atmospheric vapour pressure deficits alone (irrigated trees). Atmospheric
542 vapour pressure deficit will become an increasingly limiting factor for photosynthesis as the
543 atmosphere warms and needs to be considered explicitly in climate and land surface model
544 projections (Novick et al. 2016). We found that alleviating soil moisture limitation increased

net photosynthetic rates in the summer, but the high atmospheric VPD and air temperatures still resulted in a decrease in net carbon gain by more than 50% from spring values (Table 1, Fig. 2). However, it is interesting to note in this regard that while the soil+atmosphere stress resulted in a lower stomatal conductance on a given day, the energy partitioning as a function of g_s (or Ψ) appeared to lie on the same response curve (Fig. 7a-d) for the both atmosphere-only and soil+atmosphere deficits.

Conclusions

This study identified and quantified a range of photoprotection mechanisms that provide insight into the high productivity of a semi-arid pine forest at the dry timberline. Sustained regulated non-photochemical quenching is key for capitalising on variation in environmental conditions at diurnal, synoptic and seasonal scales, but system-level resilience of the photosynthetic system also involves reductions in chlorophyll content and increased efficiency in photorespiratory energy dissipation. Summer supplemental irrigation, relieving soil water stress, indicated a consistency in leaf-level photoprotection responses to soil- and atmospherically-derived stress on the basis of stomatal conductance and leaf water potential. These results support the potential for afforestation and sustainable forest productivity in degraded semi-arid zones that are also predicted to undergo significant drying trends in the coming century.

Acknowledgements

We thank Y. Moshe and the KKL/JNF for cooperation and logistics at the field site. Emanuela Negreanu, Ruth Ben-Meir, Hagai Sagi and Avraham Pelner provided much appreciated technical assistance for various aspects of this study, and Eyal Rotenberg is thanked for his invaluable role in maintaining the flux tower and meteorological instruments.

570 This project was supported by grants from the ISF (695/99) and the Minerva-Avron
571 Photosynthesis Center. The long-term operation of the Yatir Forest Research Field Site is
572 supported by the Cathy Wills and Robert Lewis program in Environmental Science.
573
574

References

Adams, H. D., M. J. B. Zeppel, W. R. L. Anderegg, H. Hartmann, S. M. Landhäusser, D. T. Tissue, T. E. Huxman, P. J. Hudson, T. E. Franz, C. D. Allen, L. D. L. Anderegg, G. A. Barron-Gafford, D. J. Beerling, D. D. Breshears, T. J. Brodribb, H. Bugmann, R. C. Cobb, A. D. Collins, L. T. Dickman, H. Duan, B. E. Ewers, L. Galiano, D. A. Galvez, N. Garcia-Forner, M. L. Gaylord, M. J. Germino, A. Gessler, U. G. Hacke, R. Hakamada, A. Hector, M. W. Jenkins, J. M. Kane, T. E. Kolb, D. J. Law, J. D. Lewis, J.-M. Limousin, D. M. Love, A. K. Macalady, J. Martínez-Vilalta, M. Mencuccini, P. J. Mitchell, J. D. Muss, M. J. O'Brien, A. P. O'Grady, R. E. Pangle, E. A. Pinkard, F. I. Piper, J. A. Plaut, W. T. Pockman, J. Quirk, K. Reinhardt, F. Ripullone, M. G. Ryan, A. Sala, S. Sevanto, J. S. Sperry, R. Vargas, M. Vennetier, D. A. Way, C. Xu, E. A. Yepez, and N. G. McDowell. 2017. A multi-species synthesis of physiological mechanisms in drought-induced tree mortality. Nature Ecology & Evolution **1**:1285-1291.

Adams III, W. W., and B. Demmig-Adams. 1994. Carotenoid composition and down regulation of photosystem II in three conifer species during the winter. Physiologia Plantarum **92**:451-458.

Badger, M. R., S. von Caemmerer, S. Ruuska, and H. Nakano. 2000. Electron flow to oxygen in higher plants and algae: rates and control of direct photoreduction (Mehler reaction) and rubisco oxygenase. Philosophical Transactions of the Royal Society of London B: Biological Sciences **355**:1433-1446.

Bai, J., D. H. Xu, H. M. Kang, K. Chen, and G. Wang. 2008. Photoprotective function of photorespiration in *Reaumuria soongorica* during different levels of drought stress in natural high irradiance. Photosynthetica **46**:232.

Baquedano, F. J., and F. J. Castillo. 2006. Comparative ecophysiological effects of drought on seedlings of the Mediterranean water-saver *Pinus halepensis* and water-spenders *Quercus coccifera* and *Quercus ilex*. Trees **20**:689.

Baquedano, F. J., and F. J. Castillo. 2007. Drought tolerance in the Mediterranean species *Quercus coccifera*, *Quercus ilex*, *Pinus halepensis*, and *Juniperus phoenicea*. Photosynthetica **45**:229-238.

Beis, A., and A. Patakas. 2012. Relative contribution of photoprotection and anti-oxidative mechanisms to differential drought adaptation ability in grapevines. Environmental and Experimental Botany **78**:173-183.

Björkman, O., and B. Demmig. 1987. Photon yield of O_2 evolution and chlorophyll fluorescence characteristics at 77-K among vascular plants of diverse origins. Planta **170**:489-504.

Boyer, J. S. 1982. Plant Productivity and Environment. Science **218**:443-448.

Breshears, D. D., N. S. Cobb, P. M. Rich, K. P. Price, C. D. Allen, R. G. Balice, W. H. Romme, J. H. Kastens, M. L. Floyd, J. Belnap, J. J. Anderson, O. B. Myers, and C. W. Meyer. 2005. Regional vegetation die-off in response to global-change-type drought. Proceedings of the National Academy of Sciences of the United States of America **102**:15144-15148.

Castillo, J. M., A. E. B. Casal, C. J. Luque, T. Luque, and M. E. Figueroa. 2002. Comparative field summer stress of three tree species co-occurring in Mediterranean coastal dunes. Photosynthetica **40**:49-56.

Combourieu-Nebout, N., A. Bertini, E. Russo-Ermolli, O. Peyron, S. Klotz, V. Montade, S. Fauquette, J. Allen, F. Fusco, S. Goring, B. Huntley, S. Joannin, V. Lebreton, D. Magri, E. Martinetto, R. Orain, and L. Sadori. 2015. Climate changes in the central

Mediterranean and Italian vegetation dynamics since the Pliocene. Review of Palaeobotany and Palynology **218**:127-147.
Cornic, G. 2000. Drought stress inhibits photosynthesis by decreasing stomatal aperture – not by affecting ATP synthesis. Trends in Plant Science **5**:187-188.
Cornic, G., and J. M. Briantais. 1991. Partitioning of photosynthetic electron flow between CO_2 and O_2 reduction in a C3 leaf (*Phaseolus vulgaris* L) at different CO_2 concentrations and during drought stress. Planta **183**:178-184.
Damesin, C., and S. Rambal. 1995. Field-study of leaf photosynthetic performance by a Mediterranean deciduous oak tree (*Quercus pubescens*) during a severe summer drought. New Phytologist **131**:159-167.
Demmig, B., K. Winter, A. Kruger, and F. C. Czygan. 1987. Photoinhibition and zeaxanthin formation in intact leaves - a possible role of the xanthophyll cycle in the dissipation of excess light energy. Plant Physiology **84**:218-224.
Demmig-Adams, B. 1990. Carotenoids and photoprotection in plants: A role for the xanthophyll zeaxanthin. Biochimica et Biophysica Acta **1020**:1-24.
Demmig-Adams, B., and W. W. Adams. 2006. Photoprotection in an ecological context: the remarkable complexity of thermal energy dissipation. New Phytologist **172**:11-21.
Demmig-Adams, B., C. M. Cohu, O. Muller, and W. W. Adams. 2012. Modulation of photosynthetic energy conversion efficiency in nature: from seconds to seasons. Photosynthesis Research **113**:75-88.
Eisenhut, M., A. Bräutigam, S. Timm, A. Florian, T. Tohge, A. R. Fernie, H. Bauwe, and A. P. M. Weber. 2017. Photorespiration is crucial for dynamic response of photosynthetic metabolism and stomatal movement to altered CO_2 availability. Molecular Plant **10**:47-61.
Elvira, S., R. Alonso, F. J. Castillo, and B. S. Gimeno. 1998. On the response of pigments and antioxidants of Pinus halepensis seedlings to Mediterranean climatic factors and long term ozone exposure. New Phytologist **138**:419-432.
Eppel, A., R. Shaked, G. Eshel, S. Barak, and S. Rachmilevitch. 2014. Low induction of non-photochemical quenching and high photochemical efficiency in the annual desert plant *Anastatica hierochuntica*. Physiologia Plantarum **151**:544-558.
Evans, J. R., and H. Poorter. 2001. Photosynthetic acclimation of plants to growth irradiance: the relative importance of specific leaf area and nitrogen partitioning in maximizing carbon gain. Plant Cell and Environment **24**:755-767.
Faria, T., D. Silverio, E. Breia, R. Cabral, A. Abadia, J. Abadia, J. S. Pereira, and M. M. Chaves. 1998. Differences in the response of carbon assimilation to summer stress (water deficits, high light and temperature) in four Mediterranean tree species. Physiologia Plantarum **102**:419-428.
Flexas, J., J. Bota, F. Loreto, G. Cornic, and T. Sharkey. 2004. Diffusive and metabolic limitations to photosynthesis under drought and salinity in C3 plants. Plant Biology **6**:269-279.
Flexas, J., and H. Medrano. 2002. Energy dissipation in C-3 plants under drought. Functional Plant Biology **29**:1209-1215.
Franco, A. C., and U. Lüttge. 2002. Midday depression in savanna trees: coordinated adjustments in photochemical efficiency, photorespiration, CO_2 assimilation and water use efficiency. Oecologia **131**:356-365.
Garcia-Plazaola, J. I., R. Esteban, K. Hormaetxe, B. Fernandez-Marin, and J. M. Becerril. 2008. Photoprotective responses of Mediterranean and Atlantic trees to the extreme heat-wave of summer 2003 in Southwestern Europe. Trees-Structure and Function **22**:385-392.

García-Plazaola, J. I., J. M. Olano, A. Hernández, and J. M. Becerril. 2003. Photoprotection in evergreen Mediterranean plants during sudden periods of intense cold weather. Trees **17**:285-291.
Genty, B., J. M. Briantais, and N. R. Baker. 1989. The relationship between the quantum yield of photosynthetic electron-transport and quenching of chlorophyll fluorescence. Biochimica et Biophysica Acta **990**:87-92.
Grossiord, C., S. Sevanto, I. Borrego, A. M. Chan, A. D. Collins, L. T. Dickman, P. J. Hudson, N. McBranch, S. T. Michaletz, W. T. Pockman, M. Ryan, A. Vilagrosa, and N. G. McDowell. 2017. Tree water dynamics in a drying and warming world. Plant, Cell & Environment **40**:1861-1873.
Grünzweig, J. M., I. Gelfand, Y. Fried, and D. Yakir. 2007. Biogeochemical factors contributing to enhanced carbon storage following afforestation of a semi-arid shrubland. Biogeosciences **4**:891-904.
Grünzweig, J. M., T. Lin, E. Rotenberg, A. Schwartz, and D. Yakir. 2003. Carbon sequestration in arid-land forest. Global Change Biology **9**:791-799.
Havaux, M. 1992. Stress tolerance of photosystem-II in vivo - antagonistic effects of water, heat, and photoinhibition stresses. Plant Physiology **100**:424-432.
Klein, T., S. Cohen, and D. Yakir. 2011. Hydraulic adjustments underlying drought resistance of *Pinus halepensis*. Tree Physiology **31**:637-648.
Klein, T., D. Hemming, T. B. Lin, J. M. Grunzweig, K. Maseyk, E. Rotenberg, and D. Yakir. 2005. Association between tree-ring and needle $d^{13}C$ and leaf gas exchange in *Pinus halepensis* under semi-arid conditions. Oecologia **144**:45-54.
Kornyeyev, D., A. S. Holaday, and B. A. Logan. 2004. Minimization of the photon energy absorbed by 'closed' reaction centers of photosystem 2 as a photoprotective strategy in higher plants. Photosynthetica **42**:377-386.
Kozaki, A., and G. Takeba. 1996. Photorespiration protects C3 plants from photooxidation. Nature **384**:557-560.
Kramer, D. M., and J. R. Evans. 2011. The importance of energy balance in improving photosynthetic productivity. Plant Physiology **155**:70-78.
Kramer, D. M., G. Johnson, O. Kiirats, and G. E. Edwards. 2004. New fluorescence parameters for the determination of Q_A redox state and excitation energy fluxes. Photosynthesis Research **79**:209-218.
Kromdijk, J., K. Głowacka, L. Leonelli, S. T. Gabilly, M. Iwai, K. K. Niyogi, and S. P. Long. 2016. Improving photosynthesis and crop productivity by accelerating recovery from photoprotection. Science **354**:857-861.
Kyparissis, A., Y. Petropoulou, and Y. Manetas. 1995. Summer survival of leaves in a soft-leaved shrub (*Phlomis fruticosa* L., Labiatae) under Mediterranean field conditions: avoidance of photoinhibitory damage through decreased chlorophyll contents. Journal of Experimental Botany **46**:1825-1831.
Llorens, L., J. Penuelas, and I. Filella. 2003. Diurnal and seasonal variations in the photosynthetic performance and water relations of two co-occurring Mediterranean shrubs, *Erica multiflora* and *Globularia alypum*. Physiologia Plantarum **118**:84-95.
Long, S. P., S. Humphries, and P. G. Falkowski. 1994. Photoinhibition of Photosynthesis in Nature. Annual Review of Plant Physiology and Plant Molecular Biology **45**:633-662.
Martínez-Ferri, E., L. Balaguer, F. Valladares, J. M. Chico, and E. Manrique. 2000. Energy dissipation in drought-avoiding and drought-tolerant tree species at midday during the Mediterranean summer. Tree Physiology **20**:131-138.
Maseyk, K., J. M. Grunzweig, E. Rotenberg, and D. Yakir. 2008a. Respiration acclimation contributes to high carbon-use efficiency in a seasonally dry pine forest. Global Change Biology **14**:1553-1567.

Maseyk, K. S., T. Lin, E. Rotenberg, J. M. Gruenzweig, A. Schwartz, and D. Yakir. 2008b. Physiology-phenology interactions in a productive semi-arid pine forest. New Phytologist **178**:603-616.

Míguez, F., B. Fernández-Marín, J. M. Becerril, and J. I. García-Plazaola. 2015. Activation of photoprotective winter photoinhibition in plants from different environments: a literature compilation and meta-analysis. Physiologia Plantarum **155**:414-423.

Murchie, E. H., and K. K. Niyogi. 2011. Manipulation of photoprotection to improve plant photosynthesis. Plant Physiology **155**:86-92.

Naumann, G., L. Alfieri, K. Wyser, L. Mentaschi, R. A. Betts, H. Carrao, J. Spinoni, J. Vogt, and L. Feyen. 2018. Global changes in drought conditions under different levels of warming. Geophysical Research Letters **45**:3285-3296.

Novick, K. A., D. L. Ficklin, P. C. Stoy, C. A. Williams, G. Bohrer, A. C. Oishi, S. A. Papuga, P. D. Blanken, A. Noormets, B. N. Sulman, R. L. Scott, L. Wang, and R. P. Phillips. 2016. The increasing importance of atmospheric demand for ecosystem water and carbon fluxes. Nature Climate Change **6**:1023.

Ort, D. R., and N. R. Baker. 2002. A photoprotective role for O_2 as an alternative electron sink in photosynthesis? Current Opinion in Plant Biology **5**:193-198.

Pausas, J. G., C. Blade, A. Valdecantos, J. P. Seva, D. Fuentes, J. A. Alloza, A. Vilagrosa, S. Bautista, J. Cortina, and R. Vallejo. 2004. Pines and oaks in the restoration of Mediterranean landscapes of Spain: New perspectives for an old practice - a review. Plant Ecology **171**:209-220.

Peguero-Pina, J. J., D. Sancho-Knapik, F. Morales, J. Flexas, and E. Gil-Pelegrín. 2009. Differential photosynthetic performance and photoprotection mechanisms of three Mediterranean evergreen oaks under severe drought stress. Functional Plant Biology **36**:453-462.

Peñuelas, J., F. Lloret, and R. Montoya. 2001. Severe drought effects on Mediterranean woody flora in Spain. Forest Science **47**:214.

Quézel, P. 2000. Taxonomy and Biogeography of Mediterranean Pines. Pages 1-12 *in* G. Ne'eman and L. Trabaud, editors. Ecology, Biogeography and Management of *Pinus halepensis* and *P. brutia* Forest Ecosystems in the Mediterranean Basin. Backhuys Publishers, Laiden.

Raz-Yaseef, N., E. Rotenberg, and D. Yakir. 2010. Effects of spatial variations in soil evaporation caused by tree shading on water flux partitioning in a semi-arid pine forest. Agricultural and Forest Meteorology **150**:454-462.

Rotenberg, E., and D. Yakir. 2010. Contribution of semi-arid forests to the climate system. Science **327**:451.

Ruban, A. V. 2016. Nonphotochemical chlorophyll fluorescence quenching: Mechanism and effectiveness in protecting plants from photodamage. Plant Physiology **170**:1903-1916.

Schiller, G. 2000. Ecophysiology of *Pinus halepensis* Mill. and *P. brutia* Ten. . Pages 51-65 *in* G. Ne'eman and L. Trabaud, editors. Ecology, Biogeography and Management of *Pinus halepensis* and *P. brutia* Forest Ecosystems in the Mediterranean Basin. Backhuys Publishers, Laiden.

Smirnoff, N. 1993. The role of active oxygen in the response of plants to water-deficit and desiccation. New Phytologist **125**:27-58.

Tatarinov, F., E. Rotenberg, K. Maseyk, J. Ogée, T. Klein, and D. Yakir. 2016. Resilience to seasonal heat wave episodes in a Mediterranean pine forest. New Phytologist **210**:485-496.

Tracewell, C. A., J. S. Vrettos, J. A. Bautista, H. A. Frank, and G. W. Brudvig. 2001. Carotenoid photooxidation in photosystem II. Archives of Biochemistry and Biophysics **385**:61-69.

Valentini, R., D. Epron, P. Deangelis, G. Matteucci, and E. Dreyer. 1995. *In-Situ* estimation of net CO_2 assimilation, photosynthetic electron fow and photorespiration in Turkey Oak (*Q. cerris* L.) leaves: diurnal cycles under different levels of water supply. Plant Cell and Environment **18**:631-640.

Valladares, F., I. Dobarro, D. Sanchez-Gomez, and R. W. Pearcy. 2005. Photoinhibition and drought in Mediterranean woody saplings: scaling effects and interactions in sun and shade phenotypes. Journal of Experimental Botany **56**:483-494.

Werner, C., R. J. Ryel, O. Correia, and W. Beyschlag. 2001. Effects of photoinhibition on whole-plant carbon gain assessed with a photosynthesis model. Plant Cell and Environment **24**:27-40.

Wingler, A., P. J. Lea, W. P. Quick, and R. C. Leegood. 2000. Photorespiration: metabolic pathways and their role in stress protection. Philosophical Transactions of the Royal Society of London B: Biological Sciences **355**:1517-1529.

Figure 1. Environmental conditions and plant water status at the study site. (A) Daytime average (black line) and maximum (grey line) air temperature; (B) daily average (black line) and daily total (grey line) photosynthetically active radiation (PAR); (C) daytime average (black line) and maximum (grey line) atmospheric vapour pressure deficit (*D*) and leaf *D* on measurement days (circles); (D) rainfall and (E) branch water potential measured predawn (circles) and at midday (squares) in the control (solid symbols) and irrigated (open symbols) trees. Water potential values are the mean of 3 samples, error bars are the standard error.

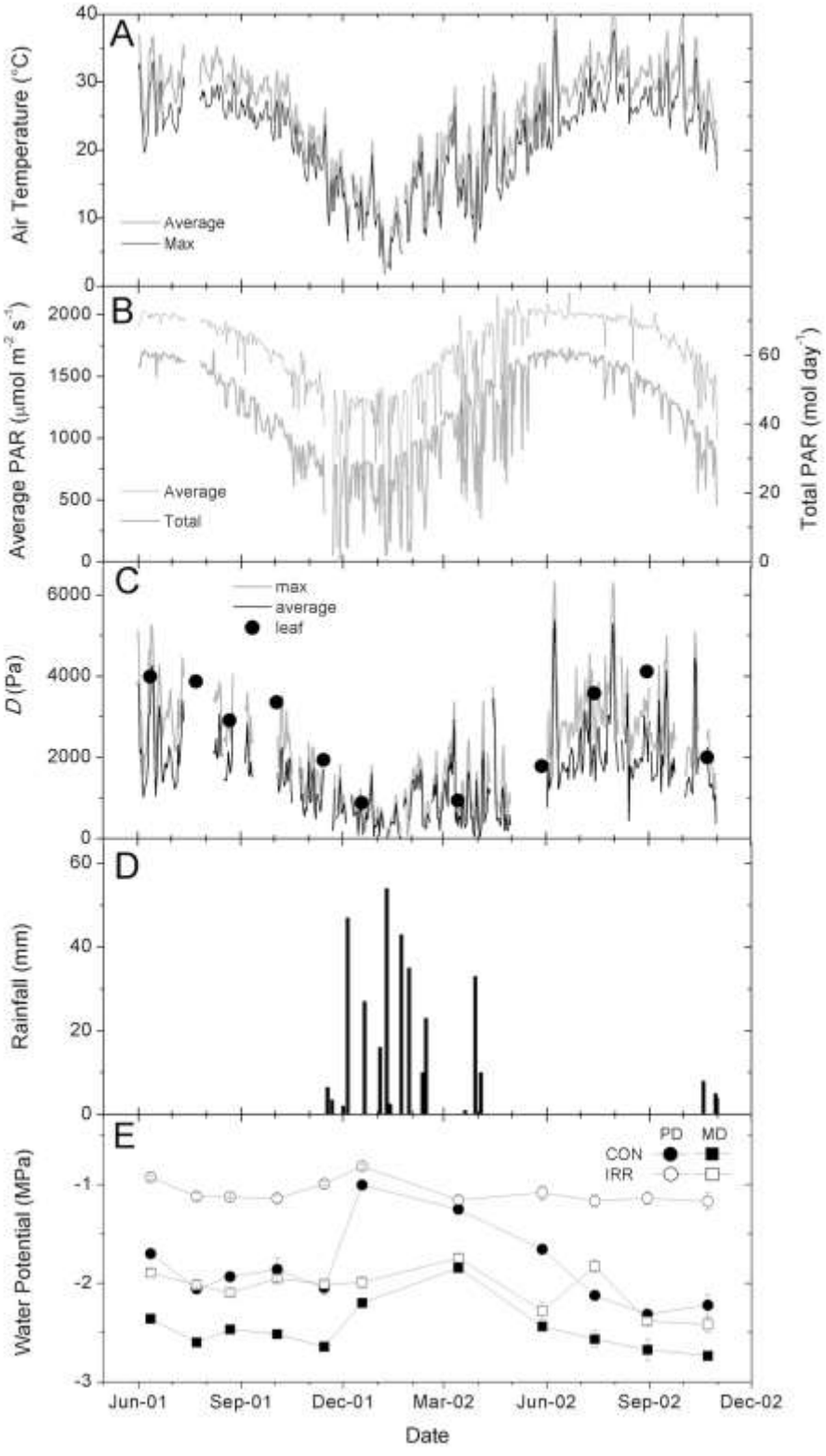

Figure 2. Representative diurnal patterns of CO_2 assimilation (A,B) and photochemical efficiency of photosystem II (Φ_{PSII}) (C,D) from different dates in the control and irrigated trees. The symbols are the same for each panel as shown in the legend in panel A.

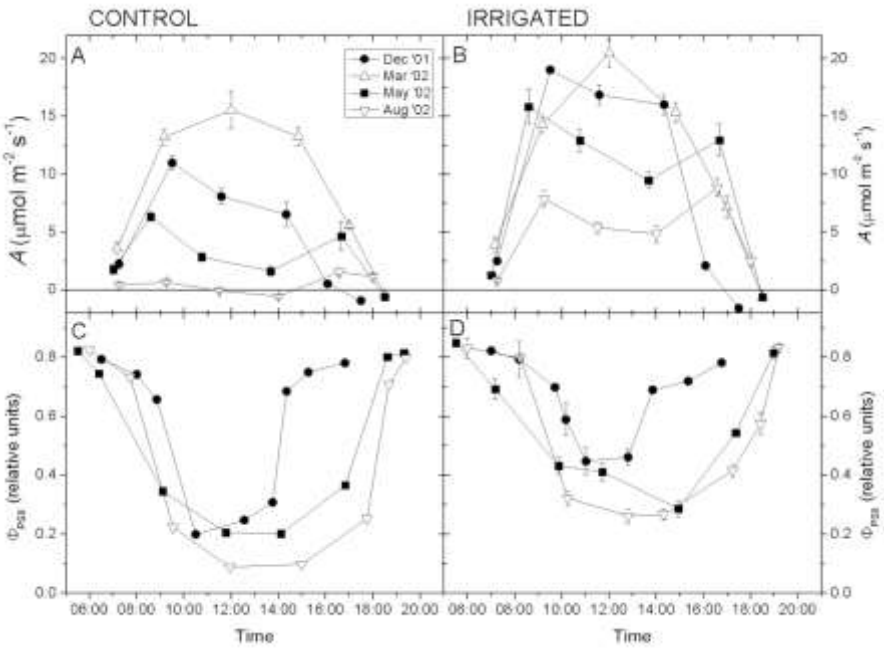

Figure 3. The relationship between assimilation rate (A) and stomatal conductance (g_s) in the control (solid symbols) and irrigated (open symbols) trees. Data is from measurements made throughout the photoperiod (for PAR > 1000 μmol m^{-2} s^{-1}) on the different measurement dates and are the average values of previous and current year needles. The fit (r^2 = 0.94) is to all data combined.

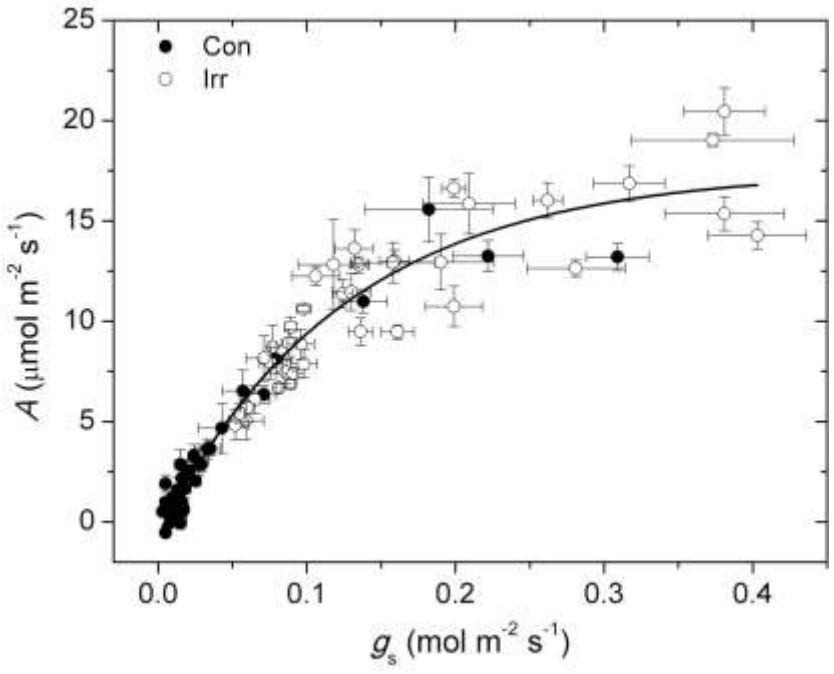

Figure 4. Diurnal time courses of the quantum efficiency of regulated thermal dissipation (Φ_{NPQ}, black circles) and constitutive dissipation (Φ_{NO}, open circles) and the de-epoxidated state of xanthophyll cycle pigments (DPS, grey squares) for control (A-C) and irrigated (D-F) trees for three dates in the year.

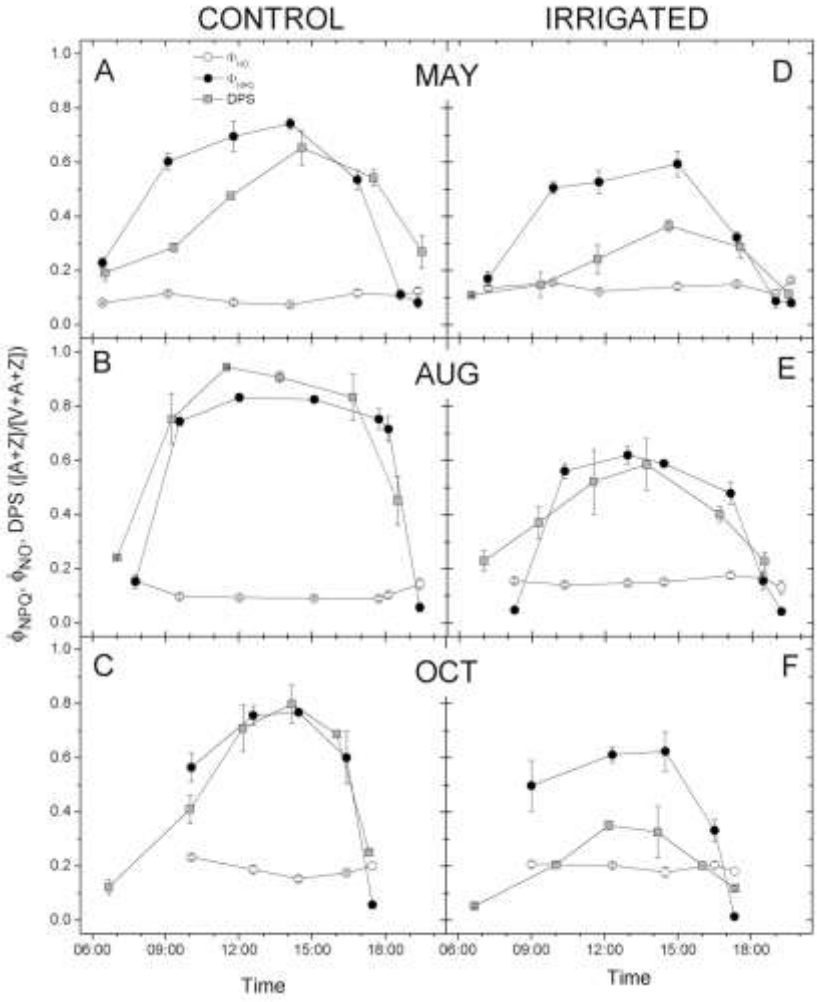

Figure 5. The proportional allocation of absorbed light energy at midday to the various photosystem dissipation pathways within in the control (left) and irrigated trees (right) across the experimental period. Open symbols, grey shading: constitutive dissipation (Φ_{NO}), open shading, grey symbols: photochemical dissipation (Φ_{PSII}), hatched shading, black symbols: regulated thermal dissipation (Φ_{NPQ}). Circles: current year (*y*0) needles, squares: previous year (*y*1) needles. The lines are through the average values of the needle age classes, and the area of shading represents the energy allocation to that pathway.

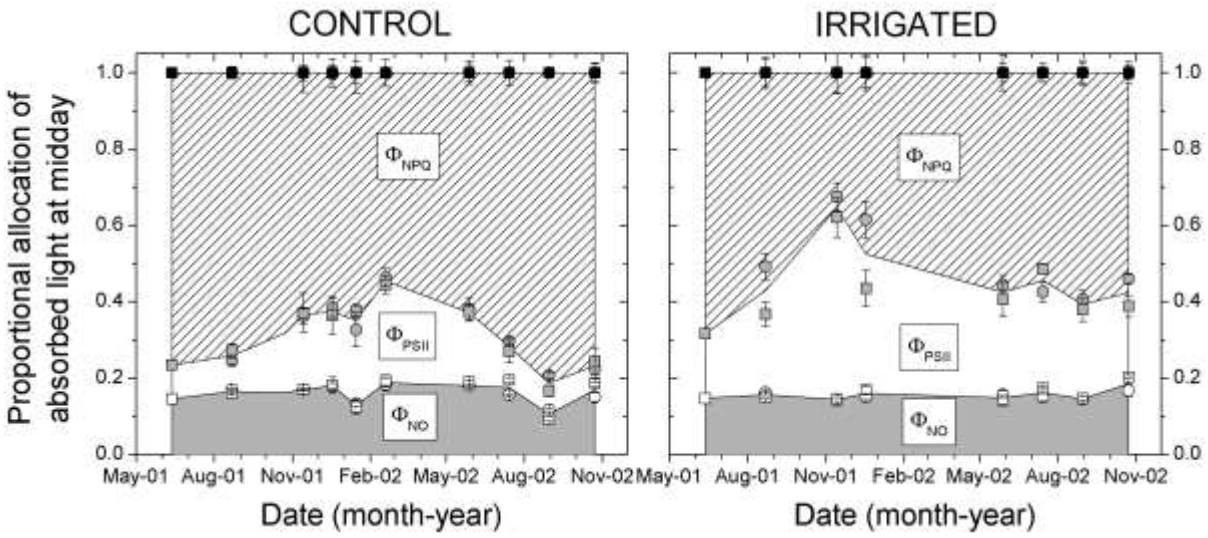

Figure 6. The dependence on photosynthetically active radiation (PAR) of electron transport rate (ETR, A), thermal dissipation rate (TDR, B) and photorespiratory CO_2 release (R_l, C) from diurnal measurements at different periods in the season. The control trees data is separated into dry season (black circles) and wet season (grey circles) data, the irrigated data (open circles) are from all dates.

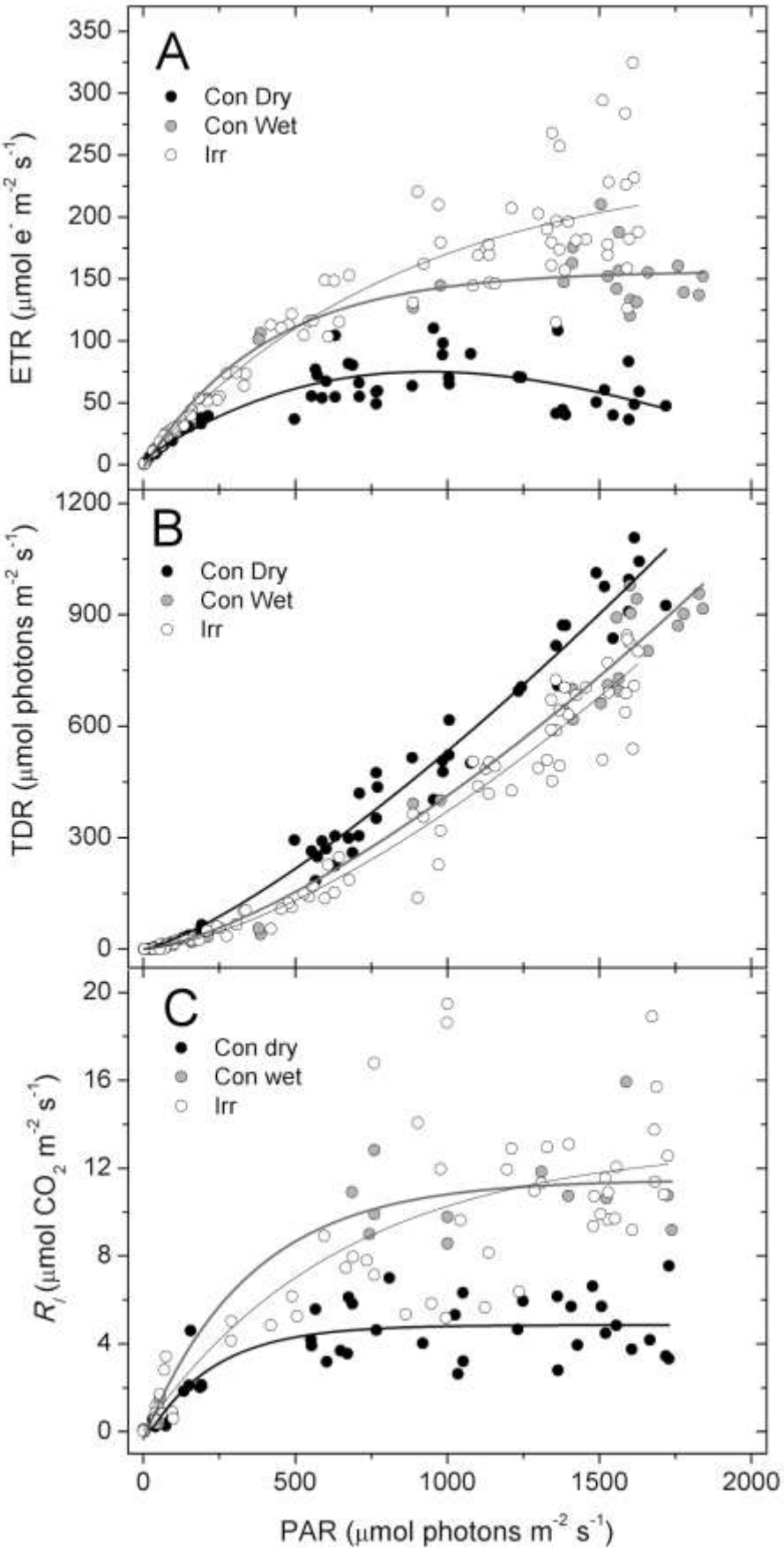

Figure 7. Relationships between energy dissipation parameters and stomatal conductance (A-D) and branch midday water potential (E-H) in the control (solid symbols) and irrigated (open symbols) trees. Proportional energy allocation is the proportion on photochemical energy allocated to CO_2 fixation (A,E) or photorespiration (B,F) or the proportion of absorbed light energy allocated to thermal dissipation (C,G). The J_o/ETR ratio is the proportion of total electron transport going to photorespiration. Fitted curves are exponential (A-D) or sigmoidal (E,F) and regression r^2 values are 0.87 (A), 0.63 (B), 0.78 (0.78), 0.91 (D), 0.75 (E) and 0.78 (F). The grey shading bars indicate the apparent threshold region in which the transition in the energy allocation patterns occur.

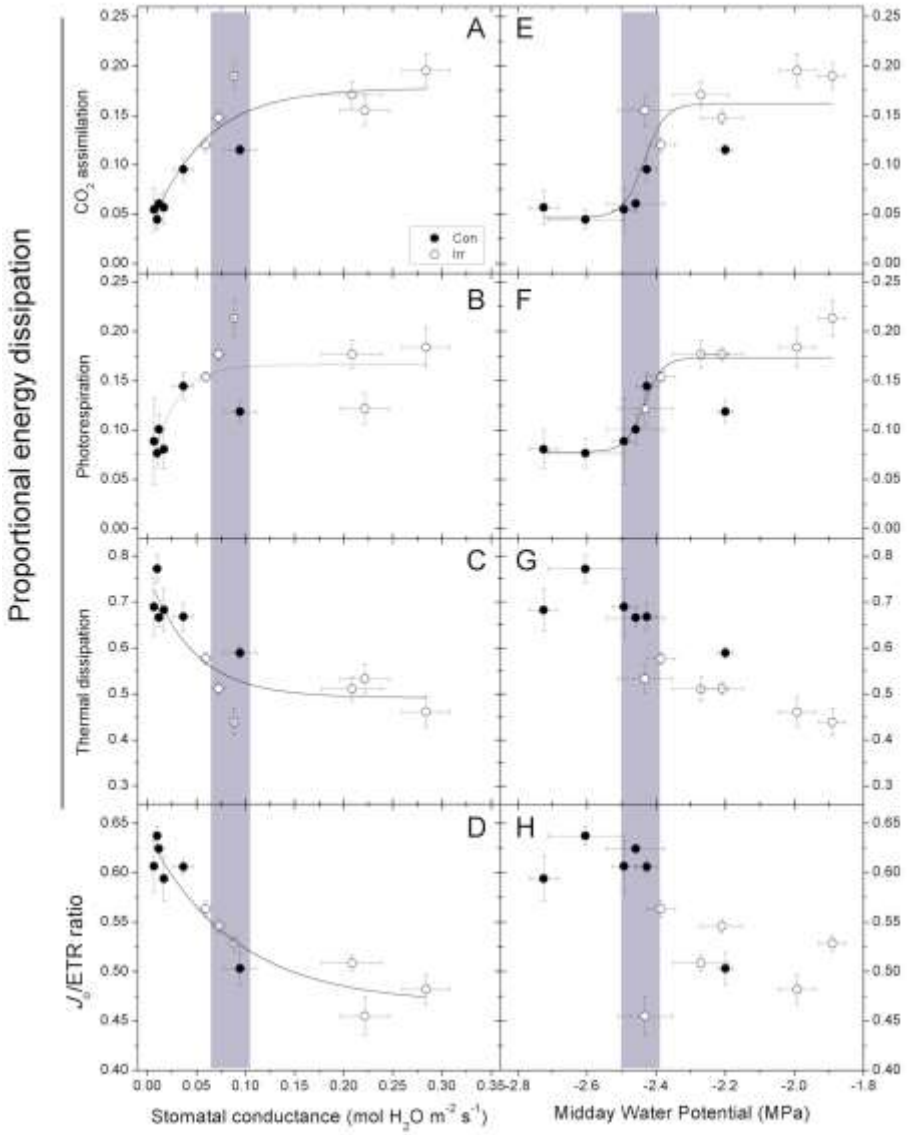

Figure 8. A schematic representation of allocation to the various energy dissipation pathways and sinks as a proportion of total daily integrated light incident on the leaf surface. The top row represents allocation during low stress and maximal CO_2 assimilation rates (irrigated trees in spring and winter) and the bottom row allocation during maximal stress and minimal CO_2 assimilation rates (summer in the control trees).

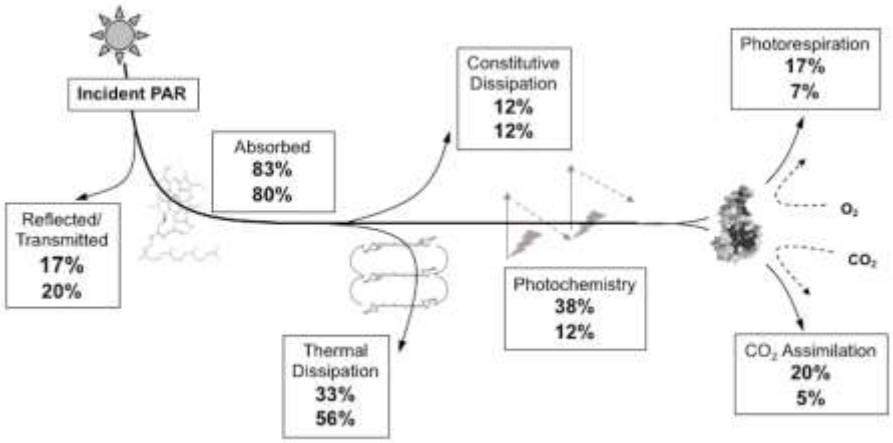

Date	Fv/Fm		Whole day PAR weighted quantum efficiency									Daily C gain (mg C m^{-2} d^{-1})
			ϕ_{PSII}			ϕ_{NPQ}			ϕ_{NO}			
Control trees												
12-Jun-01	0.804	(0.011)										185
23-Jul-01	0.803	(0.012)										102
22-Aug-01	0.825	(0.008)	0.233	(0.097)	* * *	0.600	(0.094)	* * *	0.167	(0.002)		143
14-Nov-01	0.837	(0.007)	0.249	(0.018)	* * *	0.611	(0.024)	* * *	0.140	(0.020)		108
18-Dec-01	0.802	(0.006)	0.262	(0.003)	* * *	0.562	(0.001)	* * *	0.176	(0.003)	* * *	466
14-Mar-02	0.821	(0.007)										867
28-May-02	0.823	(0.011)	0.262	(0.017)	* * *	0.642	(0.020)	* * *	0.097	(0.003)	* * *	265
14-Jul-02	0.818	(0.014)	0.182	(0.062)	* * *	0.645	(0.036)	* * *	0.173	(0.026)		84
30-	0.8	(0.0	0.1	(0.0	*	0.7	(0.0	*	0.1	(0.0	*	33

Aug-02	10	13)	21	23)	***	73	39)	***	05	16)	**	
23-Oct-02	0.796	(0.030)	0.149	(0.035)	***	0.671	(0.019)	***	0.181	(0.017)		97
						Irrigated trees						
12-Jun-01	0.814	(0.016)										669
23-Jul-01	0.833	(0.016)										562
22-Aug-01	0.850	(0.005)	0.478	(0.059)		0.358	(0.070)		0.164	(0.011)		844
14-Nov-01	0.845	(0.011)	0.573	(0.024)		0.295	(0.026)		0.133	(0.002)		655
18-Dec-01	0.823	(0.008)	0.422	(0.089)		0.417	(0.085)		0.161	(0.004)		823
14-Mar-02	0.810	(0.005)										991
28-May-02	0.813	(0.039)	0.369	(0.035)		0.487	(0.041)		0.144	(0.006)		892
14-Jul-02	0.832	(0.010)	0.336	(0.000)		0.501	(0.018)		0.163	(0.018)		505
30-Aug-02	0.831	(0.033)	0.298	(0.018)		0.550	(0.018)		0.152	(0.001)		426
23-Oct-02	0.820	(0.019)	0.293	(0.067)		0.515	(0.059)		0.192	(0.008)		632

Date	Pigment contents (mg g DW^{-1})													
	Chlorophyll (*a*+*b*)		**Total Carotenoids**		**V+A+Z**		**Neoxanthin**		**Lutein**		**a-carotene**		**b-carotene**	
							Control trees							
14-Mar-02	2.499	(0.146)	0.452	(0.025)	0.025	(0.002)	0.058	(0.039)	0.131	(0.032)	0.048	(0.027)	0.190	(0.042)
28-May-02	2.069	(0.040)	0.620	(0.017)	0.083	(0.003)	0.064	(0.035)	0.144	(0.053)	0.082	(0.124)	0.247	(0.081)
30-Aug-02	1.438	(0.031)	0.230	(0.021)	0.069	(0.005)	0.044	(0.203)	0.086	(0.137)	0.010	(0.261)	0.041	(0.282)
23-Oct-02	1.166	(0.038)	0.366	(0.031)	0.096	(0.007)	0.033	(0.066)	0.085	(0.050)	0.020	(0.210)	0.128	(0.034)
							Irrigated trees							
14-Mar-02	2.819	(0.112)	0.491	(0.036)	0.023	(0.003)	0.069	(0.048)	0.170	(0.053)	0.050	(0.076)	0.179	(0.051)
28-May-02	2.291	(0.028)	0.690	(0.025)	0.075	(0.004)	0.071	(0.063)	0.166	(0.074)	0.094	(0.103)	0.266	(0.061)
30-Aug-02	1.649	(0.011)	0.271	(0.019)	0.042	(0.004)	0.049	(0.074)	0.105	(0.073)	0.014	(0.163)	0.074	(0.170)
23-Oct-02	1.528	(0.028)	0.435	(0.023)	0.108	(0.008)	0.044	(0.046)	0.100	(0.078)	0.049	(0.202)	0.137	(0.060)

Date	Pigment ratios				
	Carotenoid/ chlorophyll	**Xanthophyll/ chlorophyll**	**Carotene/ chlorophyll**	**Xanthophyll/ carotenoid**	**Carotene/ carotenoid**
			Control trees		
14-Mar-02	0.181	0.085	0.095	0.473	0.527
28-May-02	0.299	0.141	0.159	0.470	0.530
30-Aug-02	0.160	0.138	0.036	0.864	0.222
23-Oct-02	0.314	0.184	0.127	0.586	0.405
			Irrigated trees		
14-Mar-02	0.174	0.093	0.081	0.535	0.465
28-May-	0.301	0.136	0.157	0.453	0.523

02					
30-Aug-02	0.164	0.119	0.053	0.723	0.324
23-Oct-02	0.285	0.165	0.122	0.580	0.428